International Arab Journal of Dentistry

Volume 10 | Issue 2 Article 1

10-10-2019

Effect of a novel thermal treatment on rough titanium implant surfaces – "In vitro" evaluation

Rahil DOUWEIHY

Carole CHAKAR

Georges HILAL

Zeina AL MAJZOUB

EFFECT OF A NOVEL THERMAL TREATMENT ON ROUGH TITANIUM IMPLANT SURFACES – *IN VITRO* EVALUATION

Rahil Douweihy* | Carole Chakar | Georges Hilal*** | Zeina AK Majzoub******

Abstract

Current trends in modern biomedical research target the development of dental implant surfaces that are more biocompatible, and highly osteoconductive/ osteoinductive to achieve faster osseointegration and stronger bone-to-implant interface, especially under poor local and systemic clinical conditions. Heat treatment has been suggested to alter surface characteristics and result in improved biological response.

The objectives of the present in vitro study are to evaluate the impact of a novel heat treatment method of rough titanium implants on cell viability, cell proliferation, and alkaline phosphatase activity.

Six groups of grade 4 commercially pure titanium (Ti) discs measuring 6 mm in diameter and 2 mm in thickness were obtained. Surface roughness was evaluated quantitatively and qualitatively using stylus type surface profilometer and scanning electron microscopy. Human osteosarcoma cells (SaOS-2) were seeded on all discs and cell concentration in suspension, count of viable cells and alkaline phosphatase activity (ALP) were evaluated at 3, 5 and 7 days. Multiple t-tests were used to compare the cellular parameters among pairs of groups at $p<0.05$.

Surface roughness was the lowest in the sandblasted groups followed by the sandblasted/ fluoridric acid-treated and finally by the sandblasted/ CNRS-acid treated samples. Overall, all groups showed similar levels of cell proliferation, cell count, and ALP activity with only minor non-specific significant differences.

The rapid screening of the investigated Titanium surfaces confirmed their biocompatibility and warrant further testing of the proprietary acid and heat-treated surfaces SA2T under in vivo conditions.

Keywords: Acid treatment - alkaline phosphatase - cell culture - dental implant - heat treatment - surface modification – titanium.

IAJD2019;10(2):43-53.

EFFET D'UN NOUVEAU TRAITEMENT THERMIQUE SUR LA RUGOSITÉ DE LA SURFACE D'IMPLANT EN TITANE - ÉVALUATION *IN VITRO*

Résumé

Les tendances actuelles de la recherche biomédicale moderne ciblent le développement de surfaces d'implants dentaires plus biocompatibles et hautement ostéoconductrices / ostéoinductives afin de parvenir à une ostéointégration plus rapide et à une interface os-implant plus forte, en particulier dans des conditions cliniques locales et systémiques médiocres. Il a été suggéré que le traitement thermique altère les caractéristiques de la surface et améliore la réponse biologique.

Les objectifs de la présente étude réalisée in vitro sont d'évaluer l'impact d'une nouvelle méthode de traitement thermique d'implants en titane brut sur la viabilité et la prolifération cellulaire et sur l'activité de la phosphatase alcaline.

Six groupes de disques de titane (Ti) de qualité 4, commercialement purs, mesurant 6 mm de diamètre et 2 mm d'épaisseur ont été obtenus. La rugosité de surface a été évaluée quantitativement et qualitativement en utilisant un profilomètre de surface de type stylet et une microscopie électronique à balayage. Des cellules d'ostéosarcome humain (SaOS-2) ont été ensemencées sur tous les disques et la concentration cellulaire en suspension, le nombre de cellules viables et l'activité de la phosphatase alcaline (ALP) ont été évalués à 3, 5 et 7 jours. Des tests statistiques ont été utilisés pour comparer les paramètres cellulaires parmi des paires de groupes à $p<0,05$.

La rugosité de surface était la plus faible dans les groupes sablés, suivie par les échantillons sablés / traités à l'acide fluoridrique et enfin par les échantillons traités par sablage / acides CNRS. Dans l'ensemble, tous les groupes ont présenté des niveaux similaires de prolifération cellulaire, de numération cellulaire et d'activité de la PAL, avec seulement des différences significatives non spécifiques mineures.

Le criblage rapide des surfaces en titane étudiées a confirmé leur biocompatibilité et justifie des tests supplémentaires de la surface brevetée SA2T, traitée par acide et thermiquement, dans des conditions in vivo.

Mots-clés: traitement acide - phosphatase alcaline - culture cellulaire - implant dentaire - traitement thermique - modification de surface - titane.

IAJD2019;10(2):43-53.

* DDS, PG Endo, MS Oral Biol
Dpt of Endodontics,
Faculty of Dental Medicine,
Saint Joseph University,
Beirut, Lebanon
rahildouaihy@gmail.com

** DDS, MSc, PhD
Head of Dpt of Periodontics,
Faculty of Dental Medicine,
Saint Joseph University,
Beirut, Lebanon

***PhD, DEPD, CSPQ
Ass. Prof. in Clinical Biochemistry, Cancer and Metabolism Laboratory,
Saint Joseph University,
Beirut, Lebanon

**** DCD, DMD, MScD
Prof. in Periodontology,
Faculty of Dental Medicine,
Lebanese University, Beirut,
Lebanon

Introduction

The first generation of osseointegrated titanium (Ti) dental implants has been introduced by the Brånemark group in the late 1960s and was produced by industrial machining of screw-type commercially pure Ti (cpTi) implants with minimally rough topography. Despite high clinical success rates of smooth implants in prospective clinical trials [1, 2], these implants required healing periods as long as 6 to 9 months prior to loading, and were associated with relatively high failure rates in difficult clinical situations such as poor bone quality, especially in the posterior maxilla [3]. In addition, systemic conditions that affect bone metabolism such as smoking, poorly-controlled diabetes, osteoporosis, intake of certain medications, or oncologic conditions involving the skeletal system may be associated with higher rates of implant failure [4-7]. For these reasons, biomedical research is still committed to develop implant surfaces with improved bioactivity which could accelerate bone healing, optimize bone-to-implant contact, reduce the occurrence of peri-implant bone loss, and allow re-osseointegration of an implant surface affected by bone loss (Pellegrini et al. 2018).

Generally, surface treatments aim at the formation of a thick layer of Ti oxide, at the modification of surface chemical composition, and/or at the creation of surface micro- and nano-roughness which are beneficial for osseointegration [8]. Micro-roughening and nano-roughening of machined implants can be achieved by subtractive and additive treatments. Subtractive processes consist of grit-blasting, acid-etching, electropolishing, mechanical polishing, and laser micro-texturing. Additive processes include Ti plasma-sprayed coating, hydroxyapatite (HA) and calcium phosphate coatings, oxidation, ion deposition, and sintering of Ti powder [8]. Novel surface modification strategies include photo-functionalization [9, 10], laser treatment [11, 12], electrochemical anodization with titania nanostructures [13], and calcium-phosphate coatings using electrochemical deposition [14] with incorporation of various molecules into the HA coatings such as Ti atoms (Ti-doped HA) [15], collagen-derived peptides [16], carbonates [17], and grapheme oxide/chitosan [18].

Heat treatment (HT) is a relatively simple method for surface modification of Ti to enhance surface characteristics and bioactivity. In 1996, Kokubo and his group developed a technique for obtaining a bioactive surface through alkali and HT of Ti [19-21]. The technique consists in HT after soaking in sodium hydroxide (NaOH) or HCl solution, which results in the formation of a uniform bone-like apatite bioactive layer on the Ti surface in a physiological environment, and direct bonding of Ti to living bone through this layer [19, 22]. When subjected to alkali and HT, the apatite-forming ability on the surface layer of Ti may deteriorate in high-humidity environments [23]. Subsequently, Kizuki et al. [23] and Fukuda et al. [24] developed Ca-treated Ti, in which soaking in CaCl2 solution and ultrapure water was added to the process to achieve surface stability. More recently, alkali-HT incorporates a wide range of temperatures and exposure periods as well as alkali solutions of variable concentrations [25, 26]. Mixed acid treatment of Ti surfaces has been suggested as an alternative to alkali treatment because it uses lower temperature and shorter time period [27, 28]. Autoclaving [29, 30] and rapid flow-through HT in air have also been reported [31].

HT has been demonstrated to significantly affect surface topography and crystallinity, wettability and water contact angle, surface energy of Ti, protein-adsorption and apatite-formation abilities [32-34]. HT increases the thickness of Ti dioxide, mainly in its anatase form, which favors apatite deposition [14, 31]. The thickness and gradual transformation of the titania layer from an amorphous to a crystalline state depends on the exposure period and the temperature of the air or chemical treatment [31, 32]. HT has been demonstrated to be associated with enhanced bone cell adhesion and osseointegration in cell cultures [35] and animal models [36-38].

Accompanying the current trends in modern biomedical research targeting the development of dental implant surfaces that are highly osteoconductive/ osteoinductive for improved clinical performance and using simple low cost technologies, the authors introduce novel acid- and heat- treatment methods for implant surface modification suitable for large scale, simple, and eco-friendly industrial production. The aims of the present study are to:

evaluate surface characteristics of commercially pure Ti discs modified through mechanical, chemical, and heat treatments; and

evaluate the in vitro response of osteoblast-like cells on the treated Ti discs.

Materials and methods

Sample preparation

Discs (n=1080) measuring 6 mm in diameter and 1 mm in thickness were computer-aided-design and computer-aided-manufacturing (CAD/CAM) milled with a 5-axis milling machine from grade 4 commercially pure Ti blanks (Rmedical s.r.l Unipersonale, Albignasego, Padova, Italy). All discs were sandblasted with aluminum oxide Al2O3 particles using a proprietary process and divided into 6 groups of 180 each according to the type of subsequent surface treatment (Fig. 1):

Group S (n=180): sandblasted only;
Group ST (n=180): sandblasted and thermally treated at 600°C;
Group SA1 (n=180): sandblasted with subsequent fluoridric acid treatment;
Group SA1T (n=180): sandblasted and fluoridric acid-treated with subsequent thermal treatment;
Group SA2 (n=180): sandblasted with subsequent novel CNRS acid treatment methodology; and
Group SA2T (n=180): represented by thermally-treated SA2 surfaces.

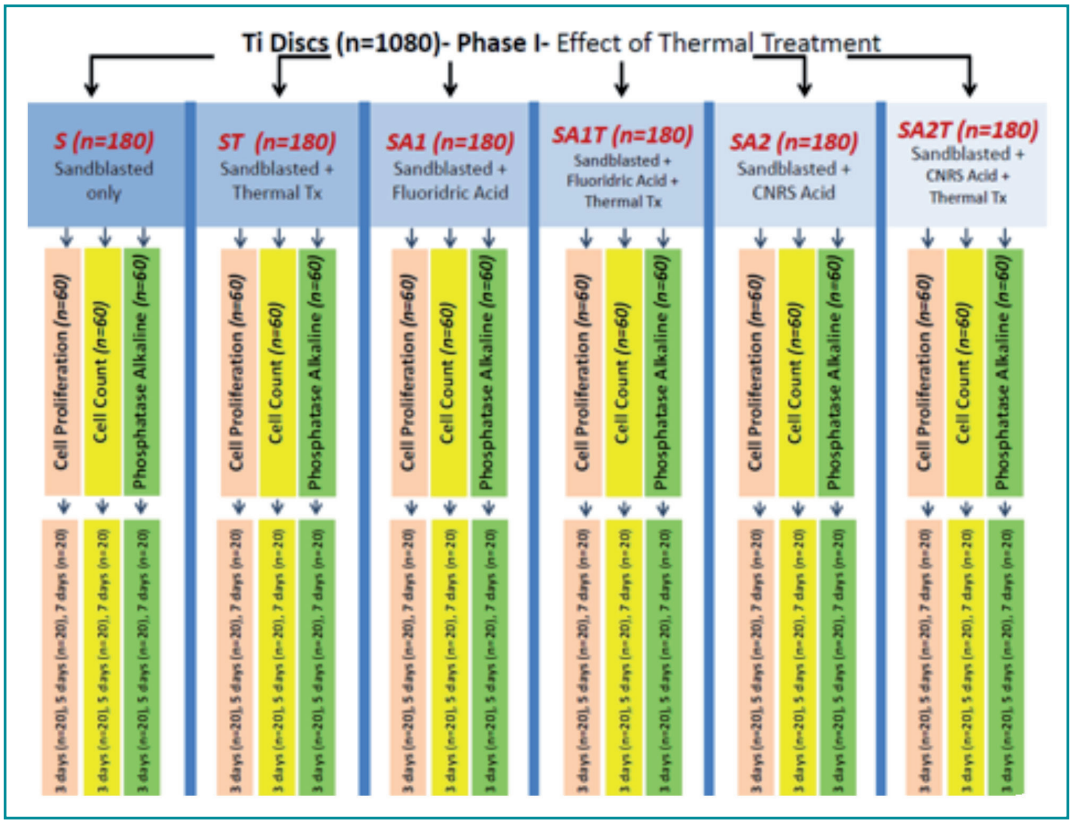

Fig. 1: Experimental design. S=sandblasted; SA1=sandblasted with fluoridric acid treatment; SA2=sandblasted with CNRS sulfuric acid treatment; ST=sandblasted and thermally treated; SA1T= SA1 surface with thermal treatment; SA2T=SA2 surface with thermal treatment.

The chemical and thermal treatment parameters are proprietary of the CNRS and their specific details were not provided by the researchers of the CNRS. After completion of the mechanical, chemical and heat surface treatments, all samples were ultrasonically degreased in acetone and ethanol for 10 minutes, and rinsed with deionized water between and after the application of each solvent. Sterilization was performed using gamma radiation at a total dose of 25 KGγ prior to in vitro testing.

Characterization of surface topography

Surface roughness measurements were carried out on larger Ti substrates subjected to the same types of treatment as the discs. The arithmetic mean deviation of the assessed profile Ra was evaluated using a stylus profilometer (KLA-Tencor Alpha-Step IQ). In addition, the samples were coated with gold-palladium using a sputter coater (MED 010 Balzers Union Carbon Coater) and the coated samples observed under a scanning electron microscope (FE-SEM, Zeiss LEO 440) with an electron beam acceleration voltage of 5 kV to assess surface topography. Photographs of the different surfaces were obtained using a magnification of x500.

Cell preparation

Human osteosarcoma cells SaOS-2 (ATCC, American Type Cell Culture, USA) were cultured in Dulbecco's Modified Eagle's Medium (DMEM) (4.5 g/L) supplemented with 10% fetal bovine serum (FBS) and 1% of penicillin/streptomycin (P/S) (Sigma-Aldrich Chemical Co., St. Louis, MO, USA) at 37°C in a humidified atmosphere with 5% CO2- 95% air incubator (Thermo Scientific Fisher, USA). The culture media were changed at 2-day intervals.

At 80% confluence, the cell monolayer was washed twice with sterile Dulbecco's phosphate-buffered saline (DPBS) (Thermo Fisher Scientific) to ensure total removal of medium and cell debris. Subsequently, cell splitting was performed using 0.05% Trypsin-EDTA (TE) (Sigma Chemical Co.) solution in PBS (Sigma Chemical Co.). The protease trypsin breaks down the proteins responsible for cell-cell and cell-matrix adherence by cleaving peptide bonds at lysine and arginine residues. The presence of divalent cations, such as calcium, which inhibits trypsin properties, is reduced by chelating it with EDTA. A small volume of 2 ml of prewarmed 0.05% TE in PBS was applied into the petri dishes containing cells which were incubated for a maximum

of 5 minutes at 37°C. Assessment of cell detachment was performed under an optical microscope (Nikon ECLIPSE TS 100) at 500 magnification. Trypsin was subsequently inactivated using a culture medium containing 10% fetal bovine serum (FBS). The cell suspension was then transferred to a centrifuge (Thermo Scientific Fisher, Model IEC CL30R) and centrifuged at 1500 rpm for 5 minutes at 25°C.

The supernatant was aspirated and cells were re-suspended in DMEM medium prior to manual counting of the viable cells to be used for the assays. The remaining cells were seeded in a new petri dish with 10 mL of DMEM medium.

Cell concentration in suspension by optical density

The Ti discs were placed, under aseptic conditions into a sterile 96-well plate (Corning Inc.) with the treated surfaces facing upward (Fig. 2). During handling, the samples were carefully held at the disk edges with sterile tweezers to avoid any damage and/or contamination of the sample surfaces.

SaOS-2 cells in DMEM medium were seeded onto the Ti discs with a density of 1×104 cells/ well for the 3 and 5 day-evaluation intervals and 5x103 for the 7-day evaluation. Wells with only DMEM medium served as controls (Fig. 2). After incubation at 37°C for 3, 5 and 7 days, the culture medium was removed and the discs rinsed 3 times with PBS in order to remove the unattached cells. Ten µL of Tetrazolium Salt, WST-1 (Sigma Chemical Co.) were added to each well and the plate was incubated for 45 minutes at 37°C. Following incubation, cell viability was assessed as the amount of reduced Formozan product which is directly proportional to the number of viable cells. Formozan accumulation was quantified by absorbance at 450 nanometers using an enzyme-linked immunoabsorbent assay ELISA microplate reader (Thermo Electron Co.). Cell concentration in the cell suspensions was expressed as optical density (OD).

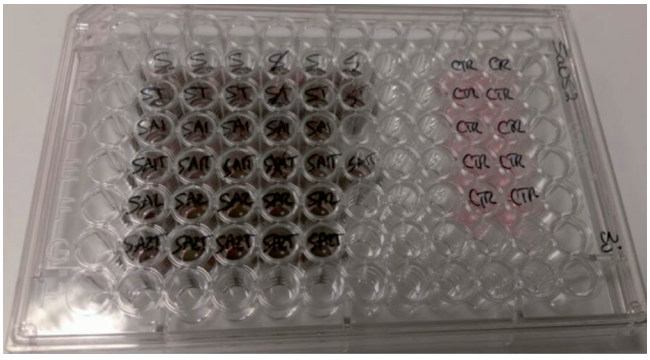

Fig. 2: The 96-well plastic plate with the Ti discs treated surfaces facing upward. Wells without discs serve as controls.

Cell count in Neubauer haemocytometer

In order to differentiate between viable and nonviable cells, the staining trypan blue method for cell counting was used. This method is based on the principle that viable cells having intact cell membrane exclude this diazo-dye, whereas the dye transverses the membrane of dead cells. As a result, viable cells have clear cytoplasm and nonviable cell has a distinctive blue color under an optical microscope. Manual cell count was performed using 10 µl of cell suspension aspirated from the wells and mixed with 40 µl of Trypan Blue (1/5 dilution ratio). Ten µl of the mixture were transferred into the chamber of a Neubauer haemocytometer and observed under a bright field optical microscope (Nikon ECLIPSE TS 100). Unstained cells were counted within each of the 4 corner squares using the following formula:

Total cell number= n x d x v x 10000

where n= the average number of cells per square,

d= dilution factor,

v= the total volume of cell suspension,

and 10000= correction factor.

Alkaline Phosphate activity (ALP) assay

ALP activity of the SaOS-2 cells was measured spectrophotometrically and quantified using a commercially availabe assay reagent kit (Alkaline Phosphatase liquicolor, HUMAN Gesellschaft für Biochemic und Diagnostica mbH, Wiesbaden, Germany). The cells were seeded onto the Ti discs placed into the 96- well plate at a density of 1×104 cells/well for 3 and 5 days, and at a density of 5x103 for 7 days with DMEM medium containing 10% FBS, ascorbate 40 g/mL and 20 g/mL β-glycerol phosphate. Five wells without discs served as control. After 3, 5 and 7 days of culture, the culture medium was removed and the cells were washed twice with PBS before cells detachment by adding trypsine. Cells were then lysed in a solution of Triton 0.1% (Triton X-100, Promega) and 1× assay buffer (RIPA buffer) and centrifuged at 1500 rpm for 5 minutes at 25°C. After centrifugation, the cell layer was suspended before removal of the lysis solution. After protein extraction, the ALP assay was performed and ALP activity was measured as the absorbance readings after 1, 2 and 3 minutes at 400 nm with a spectrophotometer (Biochrom WPA Lightwave II, USA). The calculation of ALP activity in the sample was obtained using the following formula:

$$\text{ALP (IU/L)} = \frac{\Delta\text{Abs/min} \times \text{TV} \times 1000}{18.75 \times \text{LP} \times \text{SV}}$$

Where ΔAbs/min= average absorbance change per minute

TV= total reaction volume (mL)

18.75= millimolar absorptivity of ρ-Nitrophenol

LP= light path in cm

SV= sample volume (mL)

In the study, the amount of enzyme was calculated as:

ALP (IU/L) = ΔAbs/min x 3433

Statistical Analysis

Descriptive statistics including means and standard deviations of the biological variables (optical density, cell count, ALP activity) were generated. Multiple t-tests were performed to assess the differences among pairs of groups at a significance level of $p<0.05$. The statistical analysis was performed using the Statistical Package for Social Sciences (SPSS Inc., version 17.0, Chicago, IL, USA).

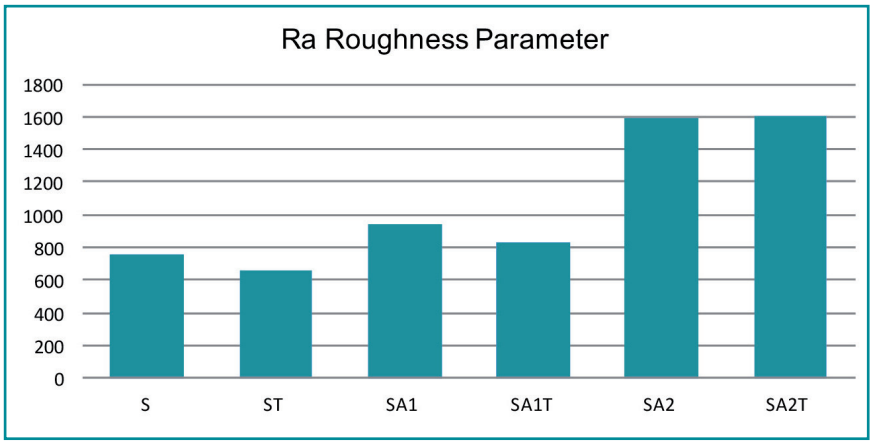

Fig. 3: Graph representing average values of the Ra roughness parameter in the 6 titanium surfaces treated. S=sandblasted; SA1=sandblasted with fluoridric acid treatment; SA2=sandblasted with sulfuric acid treatment; ST=sandblasted and thermally treated; SA1T= SA1 surface with thermal treatment; SA2T=SA2 surface with thermal treatment.

Results

Characterization of surface topography

A summary of surface roughness measurements is reported in Table 1.

The simply sandblasted samples (S and ST) showed the lowest Ra values (754±44 nm and 654±50 nm) while the acid treated ones (SA1 and SA2) were associated with higher Ra values. The sandblasted with fluoridric acid treated surface (SA1) were significantly less rough than the SA2 surfaces. The thermal treatment seemed to slightly reduce the Ra of the mechanically/chemically-treated samples. This reduction was clear for the S and SA1 samples. The impact of thermal treatment on Ra reduction was less evident for the SA2 group due to the high standard deviation (not homogeneous) within the batch.

	Ra Mean ± SD (nm)
S	754±44
ST	654±50
SA1	941±109
SA1T	836±58
SA2	1590±196
SA2T	1605±104

Table 1: Descriptive statistics of surface topography parameters in the 6 groups of surfaces. S=sandblasted; SA1=sandblasted with fluoridric acid treatment; SA2=sandblasted with CNRS sulfuric acid treatment; ST=sandblasted and thermally treated; SA1T= SA1 surface with thermal treatment; SA2T=SA2 surface with thermal treatment.

SEM-generated photos of the 6 types of surfaces are illustrated in Fig. 4.

Under SEM, the surface topography of the test groups differed from that of the control group. The sandblasted titanium discs (S) displayed a rough surface with facets produced by the blasting process with some smooth areas and other very rough sections. Topographically, the samples SA1 subjected to fluoridric acid treatment presented a two-level roughness with the largest one resulting from the sandblasting treatment and the finer one caused by the acid etching with uniformly distributed multiple shallow micropits. The SA2 surface topography was markedly more irregular with considerably deeper 3D pits. The thermal treatment introduced significant morphological changes to the Ti discs. Overall, the surface of the heat-treated groups tended to have a smoother appearance than the non-heat treated samples with a more irregular distribution of the 3D micrometric holes and darker contrast. The SA2T surface showed a highly corrugated microstructure with small and big indentations in addition to microscale pore structures.

Cell concentration

Overall, cell concentration measured by optical density was similar for all groups at the various time intervals (Table 2 and Figure 5). The only significant differences were found on day 7 between groups SA2T and SA2 ($p=0.026$) and between groups SA2 and SA1 ($p=0.015$).

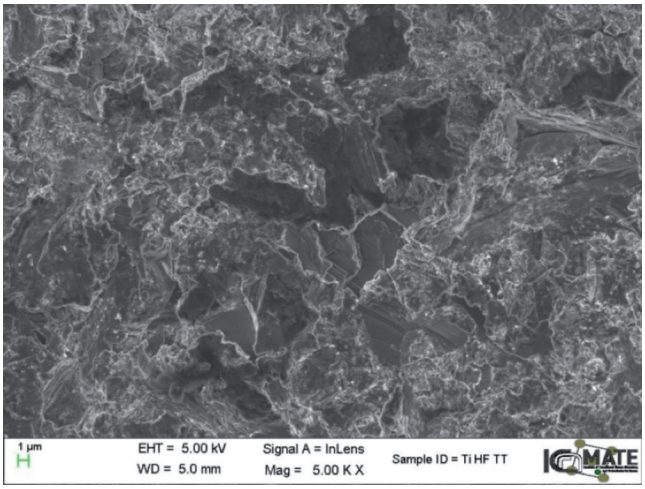

S surface

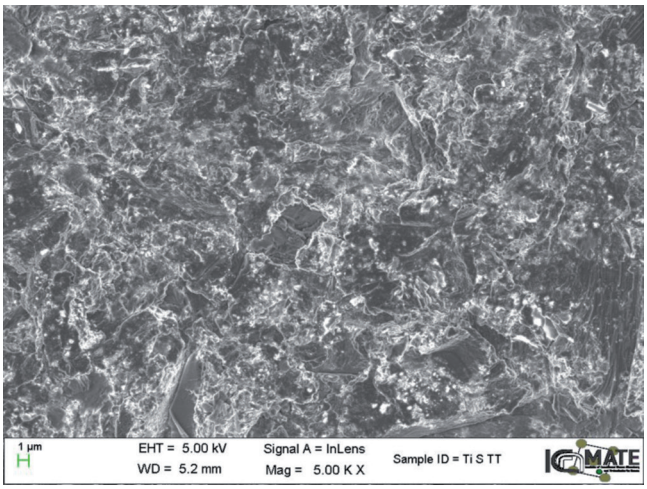

ST surface

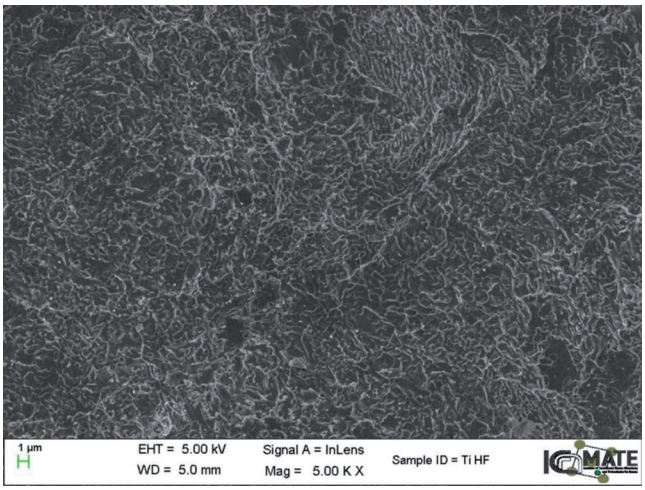

SA1 surface

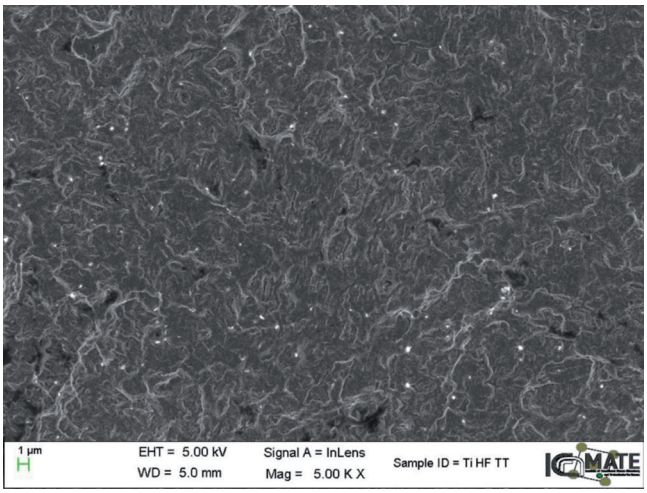

SA1T surface

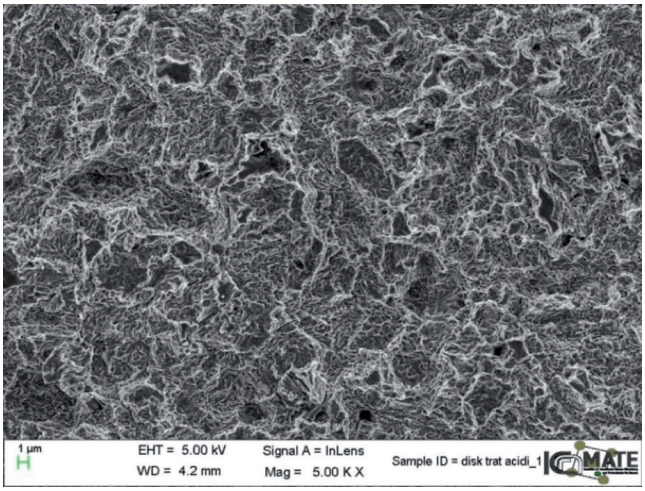

SA2 surface

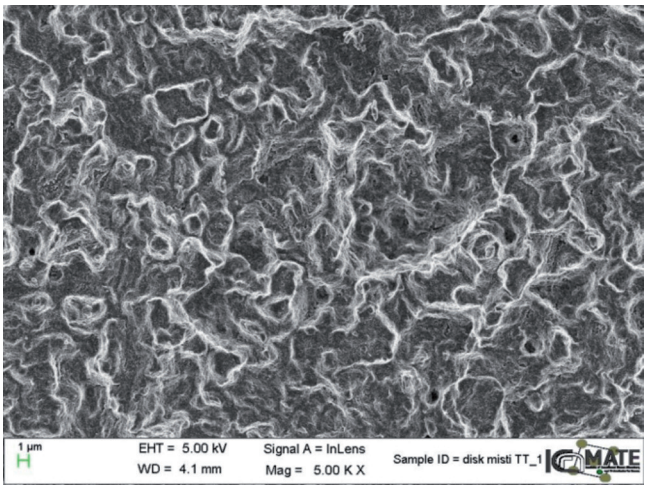

SA2T surface

Fig. 4: SEM images showing the surface topography and morphology of the titanium surfaces obtained through the 6 types of surface modification techniques: S=sandblasted ;SA1=sandblasted with fluoridric acid treatment; SA2=sandblasted with sulfuric acid treatment; ST=sandblasted and thermal treatment; SA1T= SA1 surface with thermal treatment; SA2T=SA2 surface with thermal treatment. (Original magnification x500).

Cell count

Overall, cell count was similar for all groups at the various time points (Table 3 and Figure 6). The only exceptions were for the group SA2T which exhibited significantly higher cell count at day 3 when compared with SA2 (p=0.029) and SA1T (p=0.023), and at day 5 when compared with SA1T (p=0.039).

Alkaline Phosphatase Activity

No significant differences were found between any pair of surfaces compared with the t-test (p>0.05) relative to ALP activity at days 3 and 5 (Table 4 and Figure 7). At day 7, the S group showed significantly less ALP activity than the chemically/ thermally-treated surfaces SA1T (p=0.036) and SA2T (p=0.016).

	Optical Density					
	Day 3		Day 5		Day 7	
	Mean	SD	Mean	SD	Mean	SD
S	0.721	0.243	0.548	0.161	0.527	0.105
SA1	0.552	0.054	0.562	0.164	0.584	0.036
SA2	0.516	0.115	0.566	0.156	0.468	0.033
ST	0.543	0.007	0.600	0.136	0.587	0.064
SA1T	0.566	0.239	0.647	0.203	0.511	0.123
SA2T	0.552	0.100	0.625	0.136	0.555	0.015
CTL	0.681	0.101	0.886	0.476	0.644	0.153

Table 2: Descriptive statistics with means and standard deviations of cell concentration measured by optical density according to implant surface treatment and evaluation interval. S=sandblasted; SA1=sandblasted with fluoridric acid treatment; SA2=sandblasted with sulfuric acid treatment; ST=sandblasted and thermally treated; SA1T= SA1 surface with thermal treatment; SA2T=SA2 surface with thermal treatment; CTL=control well without disc.

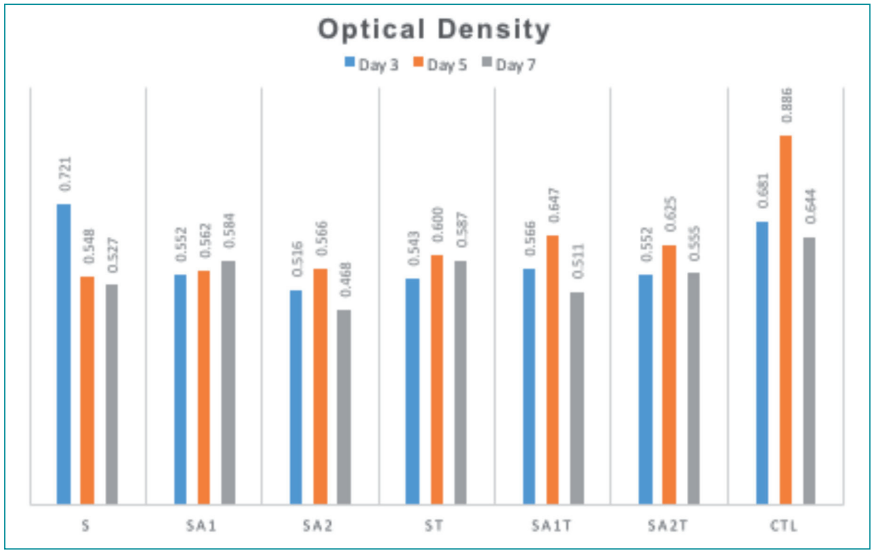

Fig. 5: Graph comparing optical density according to evaluation period and type of titanium surface treatment. S=sandblasted; SA1=sandblasted with fluoridric acid treatment; SA2=sandblasted with sulfuric acid treatment; ST=sandblasted and thermally treated; SA1T= SA1 surface with thermal treatment; SA2T=SA2 surface with thermal treatment; CTL=control well without discs.

Discussion

The purpose of the present study was to compare cellular response to 6 cpTi rough surfaces. More specifically, the type of acid treatment (A1 and A2) and proprietary heat treatment were evaluated relative to their impact on cellular concentration, cell count, and ALP activity. The results showed that all 6 surfaces were cytocompatible and supported comparable cell viability, proliferation, and ALP activity with only minor significant differences. These differences did not follow a specific pattern favoring one surface versus another except for a tendency towards greater ALP activity at day 7 for the heat-treated surfaces SA1T and SA2T when compared with the sandblasted discs (S).

In the present study, optical density of the cell suspension and cellular viability were used to evaluate Ti surface biocompatibility. These 2 tests are frequently used in vitro for rapid initial screening of biomaterials prior to further development, testing in vivo animal model and optimization for their clinical use. The study results confirmed the biocompatibility of the Ti samples treated with the proprietary acid and heat processes (SA2T) which warrant their further testing under in vivo conditions.

Cell viability is measured by determining the number of living and dead cells in a total cell sample and is an indicator of the toxic effects of tested compounds. Cell viability can be detected based on different parameters: the redox potential of the cell population, the integrity of cell membranes, or the activity of cellular enzymes such as esterases [39]. The trypan blue dye exclusion test is based on the principle that live cells possess

intact cell membranes that exclude certain dyes, such as trypan blue, eosin, or propidium, whereas dead cells do not (Strober 2001). Although trypan blue has been extensively used to determine cell viability, it has several drawbacks: trypan blue staining cannot be used to distinguish between the healthy cells and the living cells that lost their cellular functions. In addition, it has been observed that trypan blue viability measurements in samples that are lower than 70% viable show higher measured cell viability when compared to fluorescent based detection methods. Therefore, conducting viability measurements with trypan blue on samples with low viability may not be optimal. In the present study, viability was greater than 70% warranting the use of the trypan blue assay.

The 4 main techniques used for the measurement of cell proliferation rates differ according to what is measured: DNA synthesis, metabolic activity, antigens associated with cell proliferation, and adenosine triphosphate (ATP) concentration. In multi-well formats, the tetrazolium salts are widely used to assess the metabolic activities of mammalian cells and microorganisms: they are incubated with a population of viable cells to convert a substrate to a colored or fluorescent product that can be detected with a plate reader [40]. The present study evaluated metabolic cell proliferation by the water-soluble tetrazolium WST-1 colorimetric assay which uses improved tetrazolium reagents in a single-step method that eliminates a liquid handling step during the assay procedure because a second addition of reagent to the plate is not required for solubilization needed for MTT [40]. The WST-1 assay is highly sensitive (capable of detecting low cell number) and shows faster color development compared to the other salts [41].

Besides proliferation and viability, biochemical assays like ALP activity are important to associate biomaterials topography with cell differentiation [42]. ALP is an enzyme belonging to the group of membrane bound glycoproteins, and is among the first functional genes expressed in the calcification process [43]. One of the present study limitations is the evaluation of ALP at 3, 5 and 7 days without assessment at later intervals which could have revealed more significant differences among the 6 surfaces investigated. Problems related to cell confluency could not be solved. Confluent cells became very crowded with little or no space between them resulting in cellular stress with subsequent abnormal growth patterns or cell death.

In the present study a well-characterized osteoblast-like human osteosarcoma immortalized cell line SaOS-2 was used. This cell line has several advantages: ease of maintenance, unlimited number of cells without need of isolation, and relative phenotypic

	Cell Count					
	Day 3		Day 5		Day 7	
	Mean	SD	Mean	SD	Mean	SD
S	59833.33	4536.89	139833.33	19107.15	150333.33	577.35
SA1	65666.67	4041.45	126000	24248.71	145500.00	28578.84
SA2	60166.67	11094.29	97666.67	30823.42	118833.33	46060.65
ST	66966.67	8914.22	140333.33	16743.16	129433.33	13581.73
SA1T	55166.67	6525.59	130000	10000.00	116833.33	15494.62
SA2T	96666.67	15275.25	156666.67	11547.01	170333.33	26083.20
CTL	62166.67	9751.07	120866.67	27933.02	145000.00	13228.76

Table 3: Descriptive statistics with means and standard deviations of cell count according to implant surface treatment and evaluation interval. S=sandblasted; SA1=sandblasted with fluoridric acid treatment; SA2=sandblasted with sulfuric acid treatment; ST=sandblasted and thermally treated; SA1T= SA1 surface with thermal treatment; SA2T=SA2 surface with thermal treatment; CTL=control well without disc.

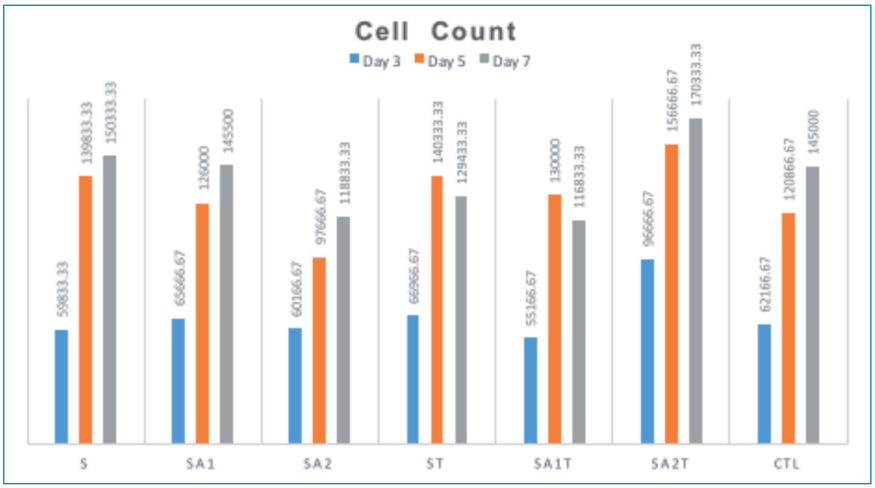

Fig. 6: Graph comparing viable cell count according to evaluation period and type of titanium surface treatment. S=sandblasted; SA1=sandblasted with fluoridric acid treatment; SA2=sandblasted with sulfuric acid treatment; ST=sandblasted and thermally treated; SA1T= SA1 surface with thermal treatment; SA2T=SA2 surface with thermal treatment; CTL=control well without disc.

	Alkaline Phosphatase Activity					
	Day 3		Day 5		Day 7	
	Mean	SD	Mean	SD	Mean	SD
S	452.23	467.01	1227.31	705.81	545.60	223.71
SA1	963.87	904.61	2060.04	751.97	1033.20	634.37
SA2	453.06	430.45	1256.10	161.23	828.55	405.55
ST	841.68	730.23	1075.51	87.92	1033.96	132.91
SA1T	685.44	481.92	1305.83	242.27	1231.54	66.58
SA2T	483.44	492.99	1101.47	195.54	1380.84	285.94
CTL	1188.25	297.43	1584.15	1007.57	857.33	345.62

Table 4: Descriptive statistics with means and standard deviations of alkaline phosphatase according to implant surface treatment and evaluation interval. S=sandblasted; SA1=sandblasted with fluoridric acid treatment; SA2=sandblasted with sulfuric acid treatment; ST=sandblasted and thermally treated; SA1T= SA1 surface with thermal treatment; SA2T=SA2 surface with thermal treatment; CTL=control well without disc.

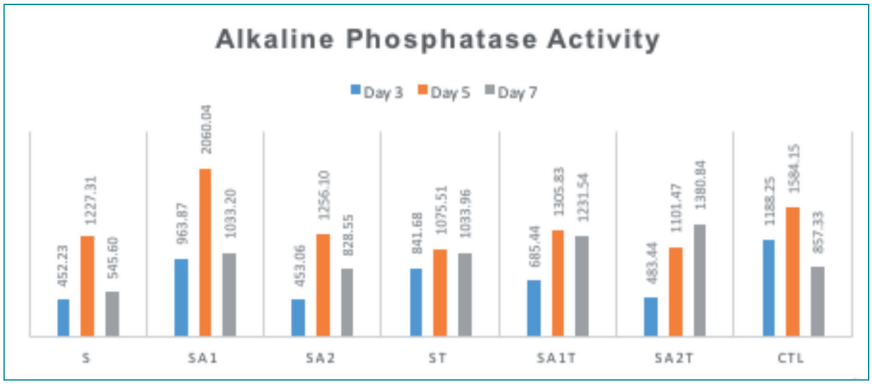

Fig. 7: Graph comparing alkaline phosphatase activity according to evaluation period and type of titanium surface treatment. S=sandblasted; SA1=sandblasted with fluoridric acid treatment; SA2=sandblasted with sulfuric acid treatment; ST=sandblasted and thermally treated; SA1T= SA1 surface with thermal treatment; SA2T=SA2 surface with thermal treatment; CTL=control well without disc.

stability [44]. This cell line is however associated with some disadvantages such as non-physiological cellular proliferation due to altered mechanisms of contact inhibition and the fact that it does not reflect the whole range of phenotypic features of normal osteoblastic cells. Although SaOS-2 cells tend to have higher levels of ALP activity than primary human osteoblast cells, the time sequential pattern of the enzyme activity has been reported to be similar [44]. In addition, collagen structure of the calcified matrix synthesized by SaOS-2 is similar to collagen formed by primary human osteoblasts although with a higher level of lysyl hydroxylation in SaOS-2 cells [45]. Furthermore, cytokine and growth factor expression of SaOS-2 cells has been shown to be comparable to primary normal osteoblastic cells [46]. The use of primary human osteoblastic cell lines is associated with large variability. Age, site of isolation and gender differences influence behavior of the cells such as the time frames for phenotypic changes in vitro [44]. The limited access of primary human osteoblasts in pathological subjects and their phenotypic heterogeneity renders their use difficult in research.

In conclusion, the results of the rapid biocompatibility screening conducted in the present study confirmed the biocompatibility of all 6 investigated rough Ti surfaces and warrant more sophisticated in vitro tests and further evaluation of the proprietary acid/heat-treated surfaces SAT2 under in vivo conditions.

References

1. Henry PJ, Laney WR, Jemt T, Harris D, Krogh PH, Polizzi G, Zarb GA, Herrmann I. Osseointegrated implants for single-tooth replacement: a prospective 5-year multicenter study. Int J Oral Maxillofac Implants. 1996;11(4):450-455.
2. Jemt T, Chai J, Harnett J, Heath MR, Hutton JE, Johns RB, McKenna S, McNamara DC, van Steenberghe D, Taylor R, Watson RM, Herrmann I. A 5-year prospective multicenter follow-up report on overdentures supported by osseointegrated implants. Int J Oral Maxillofac Implants. 1996;11(3):291-298.
3. Jaffin RA, Berman CL. The excessive loss of Branemark fixtures in type IV bone: a 5-year analysis. J Periodontol. 1991;62(1):2-4.
4. Chrcanovic BR, Albrektsson T, Wennerberg A. Smoking and dental implants: A systematic review and meta-analysis. J Dent. 2015;43(5):487-98.
5. Chrcanovic BR, Kisch J, Albrektsson T, Wennerberg A. Factors influencing early dental implant failures. J Dent Res. 2016;95(9):995-1002.
6. Chrcanovic BR, Kisch J, Albrektsson T, Wennerberg A. Analysis of risk factors for cluster behavior of dental implant failures. Clin Implant Dent Relat Res. 2017;19(4):632-642.
7. Chrcanovic BR, Kisch J, Albrektsson T, Wennerberg A. Intake of proton pump inhibitors is associated with an increased risk of dental implant failure. Int J Oral Maxillofac Implants. 2017;32(5):1097-1102.
8. Pellegrini G, Francetti L, Barbaro B, Del Fabbro M. Novel surfaces and osseointegration in implant dentistry. J Investig Clin Dent. 2018;9(4):e12349.
9. Hirota M, Ozawa T, Iwai T, Ogawa T, Tohnai I. Implant stability development of photofunctionalized implants placed in regular and complex cases: a case-control study. Int J Oral Maxillofac Implants. 2016;31(3):676-86.
10. Kitajima H, Ogawa T. The use of photofunctionalized implants for low or extremely low primary stability cases. Int J Oral Maxillofac Implants. 2016;31(2):439-447.
11. Azzawi ZGM, Hamad TI, Kadhim SA, Naji GA. Osseointegration evaluation of laser-deposited titanium dioxide nanoparticles on commercially pure titanium dental implants. J Mater Sci Mater Med. 2018;29(7):96.
12. Pires LC, Guastaldi FPS, Nogueira AVB, Oliveira NTC, Guastaldi AC, Cirelli JA. Physicochemical, morphological, and biological analyses of Ti-15Mo alloy surface modified by laser beam irradiation. Lasers Med Sci. 2019;34(3):537-546.
13. Li T, Gulati K, Wang N, Zhang Z, Ivanovski S. Bridging the gap: Optimized fabrication of robust titania nanostructures on complex implant geometries towards clinical translation. J Colloid Interface Sci. 2018;529:452-463.
14. Wang Q, Ding C, Zhou Y, Luo J, Li J. Universal and biocompatible hydroxyapatite coating induced by phytic acid-metal complex multilayer. Colloids Surf B Biointerfaces. 2018;169:478-485.
15. Nakazawa M, Yamada M, Wakamura M, Egusa H, Sakurai K. Activation of osteoblastic function on titanium surface with titanium-doped hydroxyapatite nanoparticle coating: An in vitro study. Int J Oral Maxillofac Implants. 2017;32(4):779-791.
16. Pereira KK, Alves OC, Novaes AB Jr, de Oliveira FS, Yi JH, Zaniquelli O, Wolf-Brandstetter C, Scharnweber D, Variola F, Nanci A, Rosa AL, de Oliveira PT. Progression of osteogenic cell cultures grown on microtopographic titanium coated with calcium phosphate and functionalized with a type I collagen-derived peptide. J Periodontol. 2013;84(8):1199-210.
17. Li S, Yu W, Zhang W, Zhang G, Yu L, Lu E. Evaluation of highly carbonated hydroxyapatite bioceramic implant coatings with hierarchical micro-/nanorod topography optimized for osseointegration. Int J Nanomedicine. 2018;13:3643-3659.
18. Suo L, Jiang N, Wang Y, Wang P, Chen J, Pei X, Wang J, Wan Q. The enhancement of osseointegration using a graphene oxide/chitosan/hydroxyapatite composite coating on titanium fabricated by electrophoretic deposition. J Biomed Mater Res B Appl Biomater. 2019;107(3):635-645.
19. Kokubo T, Miyaji F, Kim H-M, Nakamura T. Spontaneous formation of bonelike apatite layer on chemically treated titanium metals. J Am Ceramic Soc 1996;79:1127-1129.
20. Nishiguchi S, Nakamura T, Kobayashi M, Kim HM, Miyaji F, Kokubo T. The effect of heat treatment on bone-bonding ability of alkali-treated titanium. Biomaterials. 1999;20:491-500.
21. Nishiguchi S, Kato H, Fujita H, Oka M, Kim HM, Kokubo T, et al. Titanium metals form direct bonding to bone after alkali and heat treatments. Biomaterials. 2001;22:2525-2533.
22. Kawai T, Takemoto M, Fujibayashi S, Neo M, Akiyama H, Yamaguchi S, Pattanayak DK, Matsushita T, Nakamura T, Kokubo T. Bone-bonding properties of Ti metal subjected to acid and heat treatments. J Mater Sci Mater Med 2012;23:2981-92.
23. Kizuki T, Takadama H, Matsushita T, Nakamura T, Kokubo T. Preparation of bioactive Ti metal surface enriched with calcium ions by chemical treatment, Acta Biomater. 2010;6:2836-2842.
24. Fukuda A, M. Takemoto M, Saito T, Fujibayashi S, Neo M, Yamaguchi S, Kizuki T, Matsushita T, Niinomi M, Kokubo T, Nakamura T. Bone bonding bioactivity of Ti metal and Ti-Zr-Nb-Ta alloys with Ca ions incorporated on their surfaces by simple chemical and heat treatments. Acta Biomater 2011;7:1379-1386.
25. Hamouda IM, Enan ET, Al-Wakeel EE, Yousef MK. Alkali and heat treatment of titanium implant material for bioactivity. Int J Oral Maxillofac Implants. 2012;27(4):776-784.
26. Abdelrahim RA, Badr NA, Baroudi K. Effect of anodization and alkali-heat treatment on the bioactivity of titanium implant material (an in vitro study). J Int Soc Prev Community Dent. 2016;6(3):189-95.
27. Zhang F, Zhang CF, Yin MN, Ren LF, Lin HS, Shi GS. Effect of heat treatment on H2O2/HCl etched pure titanium dental implant: an in vitro study. Med Sci Monit. 2012;18(7):BR265-272.
28. Zhao JM, Park WU, Hwang KH, Lee JK, Yoon SY. Biomimetic deposition of hydroxyapatite by mixed acid treatment of titanium surfaces. J Nanosci Nanotechnol. 2015;15 (3):2552-2555.
29. Nakao Y, Sugino A, Tsuru K, et al. Enhancement of apatite-forming ability of parallely aligned Ti-substrates with optimum gaps by autoclaving. J Ceramic Soc of Japan. 2010;118(1378):483-486.
30. Scarano A, Crocetta E, Quaranta A, Lorusso F. Influence of the thermal treatment to address a better osseointegration of Ti6Al4V dental implants: histological and histomorphometrical study in a rabbit model. Biomed Res Int. 2018 Jun 27;2018:2349698.
31. Bhosle SM, Friedrich CR. Rapid heat treatment for anatase conversion of titania nanotube orthopedic surfaces.

Nanotechnology. 2017 Oct 6;28(40):405603. doi: 10.1088/1361-6528/aa8399. Epub 2017 Aug 2.

32. Lindahl C, Engqvist H, Xia W. Influence of surface treatments on the bioactivity of Ti. ISRN Biomaterials 2013, Article ID 205601, 13 pages.
33. Butt A, Hamlekhan A, Patel S, et al. A novel investigation of the formation of titanium oxide nanotubes on thermally formed oxide of Ti-6Al-4V. J Oral Implantol. 2015;41(5):523-531.
34. Kamo M, Kyomoto M, Miyaji F. Time course of surface characteristics of alkali- and heat-treated titanium dental implants during vacuum storage. J Biomed Mater Res B Appl Biomater. 2017;105(6):1453-1460.
35. Saldaña L, Vilaboa N, Vallés G, González-Cabrero J, Munuera L. Osteoblast response to thermally oxidized Ti6Al4V alloy. J Biomed Materials Res Part A. 2005;73(1):97-107.
36. Bodelón OG, Clemente C, Alobera MA, Aguado-Henche S, Escudero ML, Alonso MC. Osseointegration of TI6Al4V dental implants modified by thermal oxidation in osteoporotic rabbits. Int J Implant Dent. 2016;2(1) doi: 10.1186/s40729-016-0051-5.
37. Queiroz TP, de Molon RS, Souza FÁ, Margonar R, Thomazini AH, Guastaldi AC, Hochuli-Vieira E. In vivo evaluation of cp Ti implants with modified surfaces by laser beam with and without hydroxyapatite chemical deposition and without and with thermal treatment: topographic characterization and histomorphometric analysis in rabbits. Clin Oral Investig. 2017;21(2):685-699.
38. Scarano A, Crocetta E, Quaranta A, Lorusso F. Influence of the thermal treatment to address a better osseointegration of Ti6Al4V dental implants: histological and histomorphometrical study in a rabbit model. Biomed Res Int. 2018 Jun 27;2018:2349698.
39. Kwolek M, Renata M, Tecza Z. Comparison of methods used for assessing the viability and vitality of yeast cells. FEMS Yeast Res. 2014;14(7):1068-1079.
40. Riss TL, Moravec RA, Niles AL, Duellman S, Benink HA, Worzella TJ, Minor L. Cell viability assays. 2013 May 1 [Updated 2016 Jul 1]. In: Sittampalam GS, Coussens NP, Brimacombe K, et al., editors. Assay Guidance Manual [Internet]. Bethesda (MD): Eli Lilly & Company and the National Center for Advancing Translational Sciences; 2004-.
41. Smith C. Cell proliferation assays: methods for measuring dividing cells. September 25, 2012.
42. Lee YJ, Cui DZ, Jeon HR, Chung HJ, Park YJ, Kim OS, Kim YJ. Surface characteristics of thermally treated titanium surfaces. J Periodontal Implant Sci. 2012;42 (3):81-87.
43. Santiago-Medina P, Sundaram PA, Diffoot-Carlo N. The effects of micro arc oxidation of gamma titanium aluminide surfaces on osteoblast adhesion and differentiation. J Mater Sci Mater Med. 2014;25(6):1577-87.
44. Czekanska EM, Stoddart MJ, Richards RG, Hayes JS. In search of an osteoblast cell model for in vitro research. Eur Cell Mater. 2012;24:1-17.
45. Fernandes RJ, Harkey MA, Weis M, Askew JW, Eyre DR. The post-translational phenotype of collagen synthesized by SAOS-2 osteosarcoma cells. Bone. 2007;40(5):1343-1351.
46. Siddiqi A, Burrin JM, Wood DF, Monson JP. Tri-iodothyronine regulates the production of interleukin-6 and interleukin-8 in human bone marrow stromal and osteoblast-like cells. J Endocrinol. 1998;157(3):453-461.